JOURNAL OF GUIDANCE, CONTROL, AND DYNAMICS
Vol. 39, No. 5, May 2016

Engineering Notes

Composite Guidance Scheme for Impact Angle Control Against a Nonmaneuvering Moving Target

Bong-Gyun Park,* Hyuck-Hoon Kwon,† and Yoon-Hwan Kim‡
LIG Nex1, Seongnam 463-400, Republic of Korea
and
Tae-Hun Kim§
Agency for Defense Development, Daejeon 305-152, Republic of Korea

DOI: 10.2514/1.G001547

I. Introduction

IN ADVANCED guidance law designs, impact angle control has been widely required to maximize the effect of the warhead and to achieve a high kill probability. Since the first paper for impact angle control [1] was published, to the best of our knowledge, many guidance laws with impact angle constraint have been studied. Ryoo et al. [2] proposed a pure energy optimal guidance law with impact angle constraint. As an extension of this work, Ryoo et al. [3] proposed an optimal impact angle control guidance law minimizing the time-to-go weighted energy cost function. Lu et al. [4] developed three-dimensional guidance laws, which were based on proportional navigation (PN) with adaptive guidance parameters, to achieve impact angle requirements. Ratnoo and Ghose proposed a two-phase guidance law for capturing all possible impact angles against a stationary target [5] and a nonstationary nonmaneuvering target [6]. The proposed guidance law used PN with $N < 2$ for the initial phase to cover impact angles from zero to $-\pi$ through an orientation trajectory and PN with $N \geq 2$ for the final phase to intercept the target with the desired impact angle. Erer and Merttopçuoğlu [7] proposed a similar two-phase guidance law switching from biased PN to PN when the integral value of the bias met a certain value determined by engagement conditions. Most of research mentioned has focused on the impact angle as well as a zero terminal miss distance. The impact angle control, however, made the missile trajectory highly curved, which might have then missed the target within the seeker's look-angle limit. Since this leads to the mission failure, it is very important to consider the missile's physical constraints, such as the seeker's look-angle and maximum acceleration limits.

Recently, studies considering the look-angle limits as well as the impact angle have been carried out. Park et al. [8] proposed a composite guidance law comprising PN with $N = 1$ to maintain the constant look angle and PN with $N \geq 2$ to intercept the target with the desired impact angle. In [9], the error feedback loop of the look angle was included in PN with $N = 1$ for robustness and converging from the arbitrary look angle to the desired one. In [10], a pure energy optimal guidance law with an impact angle constraint and the seeker's look-angle limit was developed using optimal control theory with state variable inequality constraint. Kim et al. [11] proposed a bias-shaping method, based on the work in [7], to consider the look-angle and acceleration limits. Tekin and Erer [12] presented a two-phase guidance law with a numerical process for calculating navigation gains to handle the look-angle limits and acceleration constraints. Also, Erer et al. [13] proposed another two-phase guidance scheme to address the look-angle constraint problem, which can select an initial phase guidance law between PN and biased PN. Ratnoo [14] dealt with a similar problem to [8] and showed analytic guarantees for achieving all impact angles with any finite field-of-view (FOV) limit. These works have been studied against stationary targets, so the impact angle errors may appear at the instant of interception if the guidance laws presented in [8–14] are applied to the case of moving targets.

In this Note, a composite guidance scheme, studied in [8,9], is extended to the case of a nonmaneuvering moving target. The proposed guidance scheme is composed of modified deviated pure pursuit (DPP) with the error feedback loop of the look angle for the initial guidance phase and PN with $N \geq 3$ for the final guidance phase: the first phase is to maintain the constant look angle of the seeker, and the second is to intercept the moving target with a terminal angle constraint. The switching of guidance phases occurs when satisfying a specific line-of-sight (LOS) angle determined by engagement conditions. Guidelines on the gain tuning of modified DPP and calculation of the maximum achievable impact angle, which is calculated by taking into account the seeker's look-angle and maximum acceleration limits, are also investigated for guidance designers.

II. Characteristics of Proportional Navigation

In this section, the nonlinear equations of motion are derived in a surface-to-surface engagement. Also, the relationship between PN and impact angles [6] is described for designing a composite guidance scheme when PN guidance is implemented to intercept a nonmaneuvering moving target.

A. Problem Definition

Consider the planar engagement geometry as depicted in Fig. 1, where $X_I - O - Y_I$ is a Cartesian inertial reference frame and the subscripts M and T represent the missile and the target. V, γ, and a denote the speed, the flight-path angle, and the lateral acceleration, respectively. Also, r, λ, and γ_{M_f} are the relative range, the LOS angle, and the impact angle, respectively.

The nonlinear equations of motion in a polar coordinate system are

$$\dot{r} = V_T \cos(\gamma_T - \lambda) - V_M \cos(\gamma_M - \lambda) \tag{1}$$

$$r\dot{\lambda} = V_T \sin(\gamma_T - \lambda) - V_M \sin(\gamma_M - \lambda) \tag{2}$$

$$\dot{\gamma}_M = \frac{a_M}{V_M} \tag{3}$$

$$\sigma = \gamma_M - \lambda \tag{4}$$

where σ can be defined as the seeker's look angle under the assumption that the angle of attack (AOA) of the missile is small.

Received 26 June 2015; revision received 14 September 2015; accepted for publication 6 November 2015; published online 25 January 2016.

*Research Engineer, PGM R&D Laboratory; bgpark0615@gmail.com.
†Research Engineer, PGM R&D Laboratory; soyuz22@gmail.com.
‡Research Engineer, PGM R&D Laboratory; yhkim78@lignex1.com.
§Senior Researcher, 1st-Institute-4; tehunida@gmail.com.

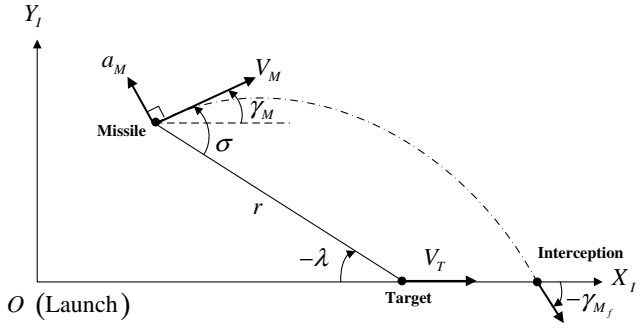

Fig. 1 Planar engagement geometry.

B. Relationship Between Navigation Gains and Impact Angles

To intercept a target, Eq. (2) should satisfy the following relationship:

$$V_M \sin(\gamma_{M_f} - \lambda_f) = V_T \sin(\gamma_T - \lambda_f) \tag{5}$$

where λ_f denotes the terminal LOS angle. From Eq. (5), at the instant of interception, λ_f is expressed as

$$\lambda_f = \tan^{-1}\left(\frac{\sin\gamma_{M_f} - \eta\sin\gamma_T}{\cos\gamma_{M_f} - \eta\cos\gamma_T}\right) \tag{6}$$

where $\eta = V_T/V_M$ and the function of $\tan^{-1}$ should be calculated from atan2, which is a four-quadrant inverse tangent function. If PN is implemented to intercept the target during the homing phase, the following relationship is satisfied as

$$\dot{\gamma}_M = N\dot{\lambda} \tag{7}$$

where N is a navigation gain. Integrating Eq. (7) with boundary conditions of γ_M and λ leads to

$$N = \frac{\gamma_{M_f} - \gamma_{M_0}}{\lambda_f - \lambda_0} \tag{8}$$

Combining Eqs. (6) and (8) yields the following relationship between N and γ_{M_f}:

$$N = (\gamma_{M_f} - \gamma_{M_0})/\left[\tan^{-1}\left(\frac{\sin\gamma_{M_f} - \eta\sin\gamma_T}{\cos\gamma_{M_f} - \eta\cos\gamma_T}\right) - \lambda_0\right] \tag{9}$$

For a nonmaneuvering moving target, the conditions [15] to generate the acceleration decreasing uniformly to zero, which can maximize the warhead effectiveness at the instant of interception due to the zero AOA for aerodynamically controlled missiles, are given as

$$1/\sqrt{2} > \eta \tag{10}$$

$$N > 2\left(1 + \eta/\sqrt{1-\eta^2}\right) > 2(1+\eta) \tag{11}$$

Since a surface target, such as a tank, moves slower than a missile, we assume $\eta \le 1/3$ in this Note. Using Eqs. (10) and (11) with $\eta \le 1/3$, N to maximize the effect of the warhead can be assumed as

$$N \ge 3 \tag{12}$$

If a surface-to-surface engagement is assumed (that is, $\gamma_T = 0$ or 180 deg and $\lambda_0 = 0$), Eq. (9) is expressed as

$$\frac{\sin\gamma_{M_f}}{\cos\gamma_{M_f} \mp \eta} = \tan\left(\frac{\gamma_{M_f} - \gamma_{M_0}}{N}\right) \tag{13}$$

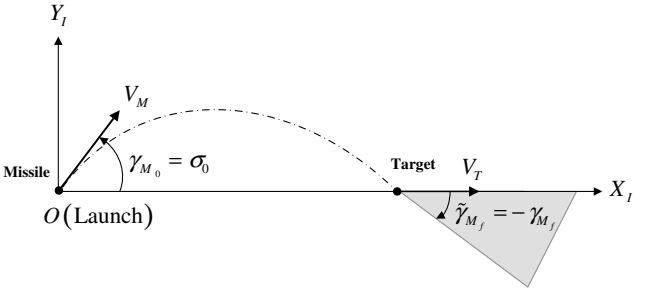

Fig. 2 Region of achievable impact angles using only PN.

where $-\eta$ at $\gamma_T = 0$ and $+\eta$ at $\gamma_T = 180$ deg. Also, if $N \to \infty$ and Eq. (13) is expressed with respect to γ_{M_f}, we have

$$\gamma_{M_f} = 0 \tag{14}$$

Hence, as shown in Fig. 2, if $N \ge 3$ from Eq. (12) and $\tilde{\gamma}_{M_f}$ is the solution of Eq. (13), the region of achievable impact angles using only PN is given by

$$\gamma_{M_f} \in [-\tilde{\gamma}_{M_f} \quad 0] \tag{15}$$

III. Composite Guidance Scheme for Impact Angle Control

In this section, a composite guidance scheme, based on characteristics of PN, with an impact angle constraint is proposed for a nonmaneuvering moving target. Under physical constraints, such as seeker's look-angle limits and acceleration capability, calculation methods of the maximum achievable impact angle and the gain selection of the proposed guidance scheme are described for a guideline for operating the missile with the limited look angle of the seeker.

A. Composite Guidance Scheme

By expressing Eq. (8) with respect to λ_0, we have

$$\lambda_0 = \lambda_f - \frac{\gamma_{M_f} - \gamma_{M_0}}{N} \tag{16}$$

Here, assuming λ_0 as λ_s that is the LOS angle at the specific instant during the homing phase and then using Eqs. (4) and (6), we have

$$\lambda_s = \left[\tan^{-1}\left(\frac{\sin\gamma_{M_f} - \eta\sin\gamma_T}{\cos\gamma_{M_f} - \eta\cos\gamma_T}\right) - \frac{\gamma_{M_f} - \sigma_d}{N}\right]\left(\frac{N}{N-1}\right) \tag{17}$$

Equation (17) means that, if the seeker look angle is maintained as the desired one σ_d within the maximum one in the initial phase and PN with $N \ge 3$ is implemented in the final phase after satisfying Eq. (17), the missile can intercept the target with an impact angle constraint outside the range of Eq. (15) (i.e., $\gamma_{M_f} \in [-\pi, \quad -\tilde{\gamma}_{M_f}]$). A switching condition λ_s depends on three main parameters, such as the desired look angle, the impact angle, and the navigation gain. Figure 3 shows that the switch condition for $\eta = 1/3$ can be satisfied for the entire range of the three parameters. Also, it can be seen that the switch condition is achieved earlier by setting the higher FOV limit or the lower navigation gain. In the case of $\eta < 1/3$, similar results can be obtained; if $\eta = 0$ (i.e., $V_T = 0$), then the results are identical to the switch condition variations described in [14].

The guidance law maintaining the constant look angle can be designed using the following differential equation of Eq. (4):

$$\dot{\sigma} = \dot{\gamma}_M - \dot{\lambda} = \frac{a_M}{V_M} - \dot{\lambda} \tag{18}$$

From $\dot{\sigma} = 0$ in Eq. (18), a look-angle maintaining guidance law is given as

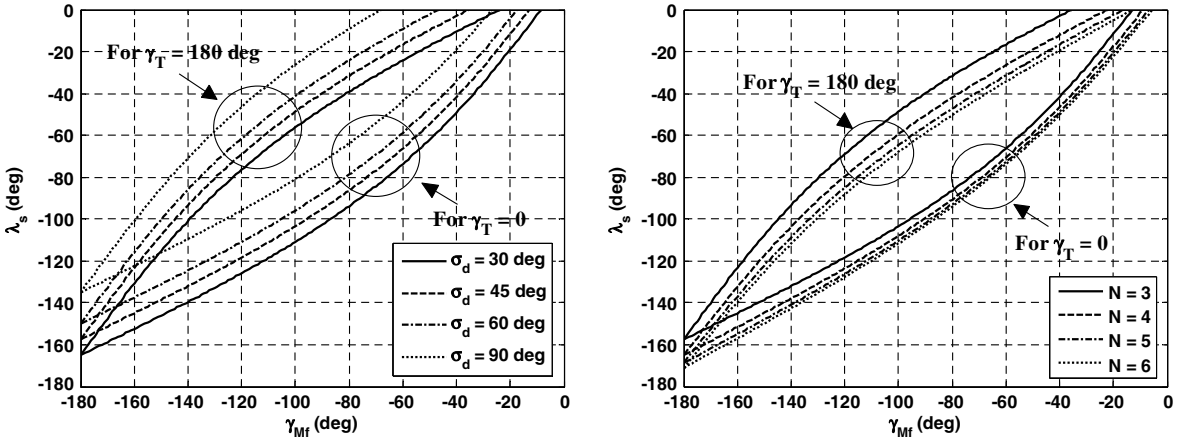

a) Different σ_d with $N = 3$ b) Different N with $\sigma_d = 45$ deg

Fig. 3 Characteristics of a switching condition λ_s for $\eta = 1/3$.

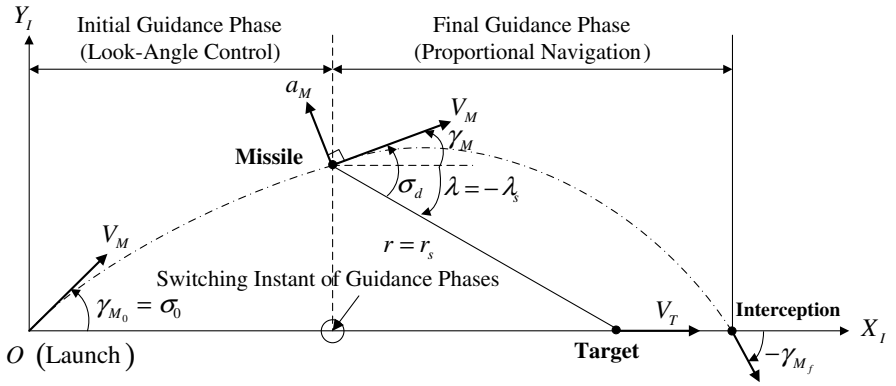

Fig. 4 Composite guidance scheme for impact angle control.

$$a_M = V_M\dot{\lambda} \tag{19}$$

where Eq. (19) was already known as pure pursuit (PP) when $\sigma = 0$ or DPP when $\sigma \neq 0$ [16]. However, if Eq. (19) is directly applied to a practical missile with noise in the look-angle measurements and system lag, the seeker could not keep the look-angle constant during the homing phase due to these error sources. Therefore, we propose a modified DPP with the error feedback loop of the look angle, called a look-angle control guidance law; that is,

$$a_{\mathrm{INI}} = V_M\dot{\lambda} + K(\sigma_d - \sigma) \tag{20}$$

where the subscript INI denotes the initial phase, and K is a proportional gain of the look-angle error. From these results, as illustrated in Fig. 4, the composite guidance scheme is proposed as

$$a_M = \begin{cases} V_M\dot{\lambda} + K(\sigma_d - \sigma) & \text{for } |\lambda| < |\lambda_s| \\ NV_M\dot{\lambda} \quad \text{with} \quad N \geq 3 & \text{for } |\lambda| \geq |\lambda_s| \end{cases} \tag{21}$$

The typical acceleration profiles of Eq. (21) are shown in Fig. 5, and their characteristics will be described in more detail in the next subsections.

B. Maximum Achievable Impact Angle

Since missiles are subject to physical constraints, such as the maximum look angle and the acceleration capability, the achievable impact angle is limited. As shown in Fig. 5, if only DPP with $\sigma_0 = \sigma_d$ is implemented for the initial phase and the LOS rate with negative values strictly decreases until the switch condition λ_s is satisfied, then the maximum magnitude of acceleration is generated at the switching instant of guidance phases because PN with $N \geq 3$, which generates the command decreasing uniformly to zero by Eqs. (10) and (11), is applied to the final phase.

Proposition 1: Satisfying $\sin^{-1}\eta < \sigma_d < \cos^{-1}2\eta$ and implementing DPP with $\sigma_0 = \sigma_d$ for the initial phase, the LOS rate $\dot{\lambda}$ with negative values strictly decreases until the switching condition λ_s is reached; that is, $\ddot{\lambda} < 0 \forall t \in [t_0, t_s]$, where t_s is the switching time of guidance phases.

Proof: Differentiating Eq. (2) with respect to t, we can obtain

$$\ddot{\lambda} = -\frac{[\dot{r}\dot{\lambda} + V_T\cos(\gamma_T - \lambda)\dot{\lambda}]}{r} \tag{22}$$

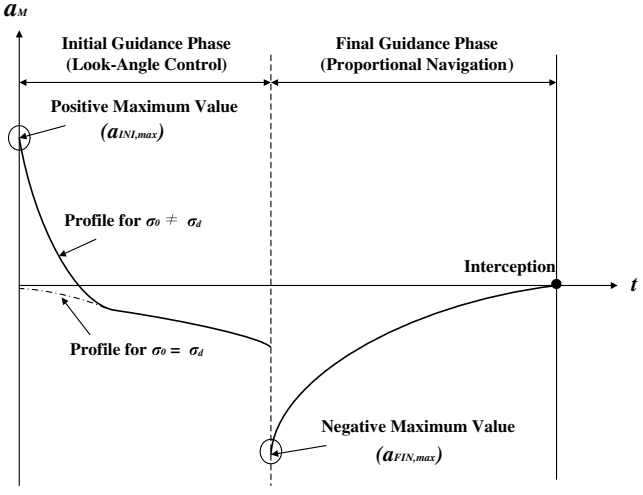

Fig. 5 Typical acceleration profiles.

Substituting Eqs. (1) and (2) into Eq. (22) leads to

$$\ddot{\lambda} = -\left(\frac{V_M}{r}\right)^2 \{[2\eta\cos(\gamma_T-\lambda)-\cos\sigma_d][\eta\sin(\gamma_T-\lambda)-\sin\sigma_d]\} \tag{23}$$

Since $(V_M/r)^2 > 0$, to guarantee $\ddot{\lambda} < 0$, the following two conditions should be satisfied:

$$2\eta\cos(\gamma_T-\lambda)-\cos\sigma_d > 0 \quad \text{and} \quad \eta\sin(\gamma_T-\lambda)-\sin\sigma_d > 0 \tag{24}$$

or

$$2\eta\cos(\gamma_T-\lambda)-\cos\sigma_d < 0 \quad \text{and} \quad \eta\sin(\gamma_T-\lambda)-\sin\sigma_d < 0 \tag{25}$$

By $|\sin\lambda|_{\max} = |\cos\lambda|_{\max} = 1$ for $\lambda \in [-\pi, 0]$ and $\gamma_T = 0$ or 180 deg, it can be concluded that

$$\sin^{-1}\eta < \sigma_d < \cos^{-1}2\eta \tag{26}$$

□

We assume Eq. (26) in our domain of interest to analytically obtain guidance parameters. Therefore, if the desired look angle is chosen to satisfy Eq. (26), we have

$$a_{FIN,\max} = \left| -N\frac{V_M^2(\sin\sigma_d \pm \eta\sin\lambda_s)}{r_s}\right| \tag{27}$$

where the subscript FIN denotes the final phase, and r_s denotes the relative range at the switching instant of the guidance phases.

Let us assume $\sigma = \sigma_0 = \sigma_d \neq 0$ in the initial phase, $\gamma_T = 0$ or 180 deg, and $|\sigma_d| < 90$ deg, considering the practical missile system. Dividing Eq. (2) by Eq. (1) yields

$$\frac{\mathrm{d}\lambda}{\mathrm{d}r} = -\frac{\tan\sigma_d\,\xi_1\,\sin\lambda \pm 1}{r\quad \xi_2\,\cos\lambda \mp 1} \tag{28}$$

where $\xi_1 = \eta/\sin\sigma_d$ and $\xi_2 = \eta/\cos\sigma_d$. The solution of Eq. (28) is given as

$$r = \frac{r_0}{[1+\xi_1\,\sin(\pm\lambda)]} e^{1/\tan\sigma_d \int_0^\lambda 1/[1+\xi_1\,\sin(\pm\lambda)]\,\mathrm{d}\lambda} \tag{29}$$

where the integral of $\int_0^\lambda 1/[1+\xi_1\,\sin(\pm\lambda)]\mathrm{d}\lambda$ can be obtained as the condition of ξ_1; that is,

$$\int_0^\lambda \frac{1}{1+\xi_1\,\sin(\pm\lambda)}\,\mathrm{d}\lambda = \begin{cases} \pm\frac{2}{\sqrt{1-\xi_1^2}}\left\{\tan^{-1}\left[\frac{\tan(\pm\lambda/2)+\xi_1}{\sqrt{1-\xi_1^2}}\right]-\tan^{-1}\frac{\xi_1}{\sqrt{1-\xi_1^2}}\right\} & \text{for } \xi_1 < 1 \\ \pm\frac{1}{\sqrt{\xi_1^2-1}}\ln\left[\frac{\tan(\pm\lambda/2)\left(\xi_1+\sqrt{\xi_1^2-1}\right)+1}{\tan(\pm\lambda/2)\left(\xi_1-\sqrt{\xi_1^2-1}\right)+1}\right] & \text{for } \xi_1 > 1 \\ \pm\left[1-\tan(\pi/4\mp\lambda/2)\right] & \text{for } \xi_1 = 1 \end{cases} \tag{30}$$

Hence, substituting Eq. (29) with Eq. (30) into Eq. (27), we obtain the following result with respect to the maximum acceleration limit $a_{\max}$:

$$a_{\max} = \frac{\mathrm{N}V_M^2[\sin\sigma_d \pm \eta\sin\lambda_s]}{\frac{r_0}{[1+\xi_1\sin(\pm\lambda_s)]} e^{\frac{1}{\tan\sigma_d}\int_0^{\lambda_s}\frac{1}{1+\xi_1\sin(\pm\lambda)}d\lambda}} \tag{31}$$

where λ_s is calculated from Eq. (17). If the right-hand side (RHS) of Eq. (31) is defined as Γ, we have

$$f(\gamma_{M_f}, a_{\max}, N, V_M, \sigma_d, r_0, V_T, \gamma_T) = a_{\max} - \Gamma = 0 \tag{32}$$

Therefore, γ_{M_f} satisfying Eq. (32) becomes the maximum achievable impact angle. Although Eq. (32) is a complicated nonlinear equation to obtain an analytical solution, the maximum impact angle $\gamma_{M_f,\max}$, which does not violate the seeker's look-angle and maximum acceleration limits, can be easily calculated by a numerical method such as the Newton–Rapshon method.

C. Gain Selection of Modified DPP

As shown in Fig. 5, the initial look angle can be set to an arbitrary angle within the maximum one. In this case, the look-angle control guidance of Eq. (20) should make the initial look angle σ_0 converge the desired one σ_d to satisfy Eq. (17). When selecting K of Eq. (20), two cases should be considered: the first is that the switching of guidance phases should occur by quickly converging to σ_d; and the second is to generate the guidance commands within $a_{\max}$.

Now, let us consider the first case. Substituting Eq. (20) into Eq. (18) yields

$$\dot{\sigma} = \frac{K}{V_M}(\sigma_d - \sigma) \tag{33}$$

and its solution is

$$\sigma(t) = \sigma_d(1 - e^{-t/\tau}) \tag{34}$$

where $\tau = V_{M/K}$, and $\sigma(t)$ converges exponentially to σ_d with τ. If $t = 5\tau$, then $\sigma = 0.99\sigma_d$. That is, the time condition of $t_s \geq 5V_M/K$ should be satisfied to implement the proposed guidance scheme.

Next, if $\sigma_0 \neq \sigma_d$, the maximum acceleration, which has a positive value, in the initial phase can be generated at the beginning of the engagement, at which the missile is far away from the target, because the LOS rate is negligible and the second term on the RHS of Eq. (20) is more dominant; that is,

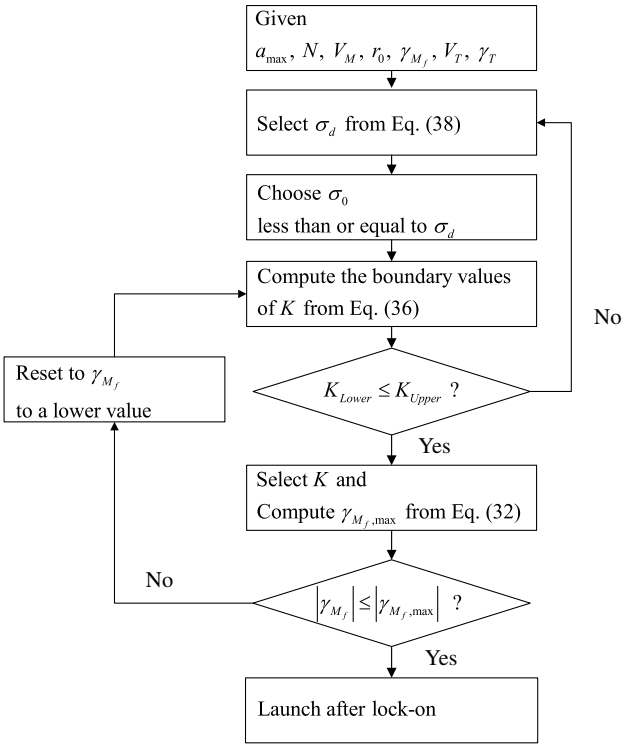

Fig. 6 Missile launch procedure using the proposed guidance scheme.

$$a_{\mathrm{INI,max}} = -\frac{V_M^2 \sin\sigma_0}{r_0} + K(\sigma_d - \sigma_0) \tag{35}$$

Therefore, to generate a_M within $a_{\max}$ in the initial phase, K should be selected by satisfying

$$\frac{5V_M}{t_s}(= K_{\mathrm{Lower}}) \le K \le \frac{\alpha_{\max} r_0 + V_M^2 \sin\sigma_0}{r_0(\sigma_d - \sigma_0)}(= K_{\mathrm{upper}}) \tag{36}$$

where t_s can be approximately calculated from a flight time equation of DPP described in [16] because the look angle in the initial phase is constant most of the time. That is,

$$t_s \approx \pm\frac{r_0}{V_r}\frac{\cos\sigma_d \pm 1/\eta - r_s/r_0[\cos(\sigma_d - \lambda_s) \pm 1/\eta]}{[(1/\eta)^2 - 1]\cos\sigma_d} \tag{37}$$

Note that, if Eq. (36) is not satisfied, the look-angle parameters should be reset to a smaller σ_d or a higher σ_0 ($\le \sigma_d$).

D. Desired Look-Angle Selection of Modified DPP

If a higher desired look angle is chosen for the initial phase, more efficient impact angle control is possible because the transverse velocity of Eq. (2) is more increased than the radial velocity of Eq. (1). However, in practical homing missiles, the look angle is limited by the seeker. Also, as shown in Fig. 3, since a high switching LOS angle of Eq. (17) is needed to achieve high impact angles, missile

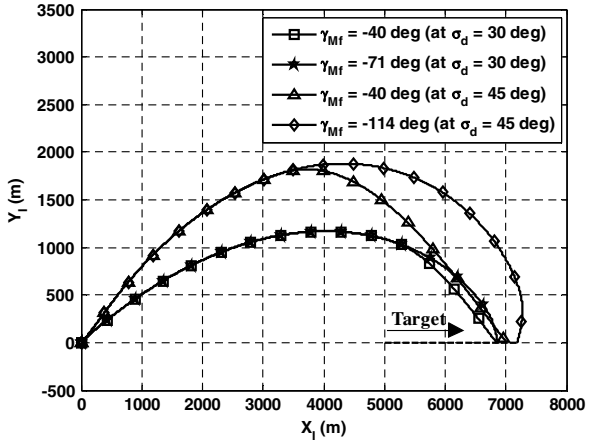

a) Missile trajectories

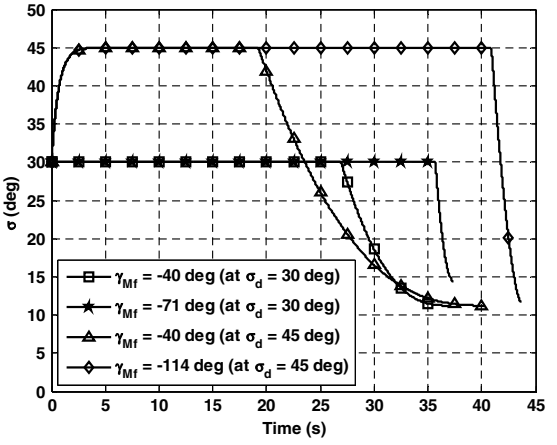

b) Look angles

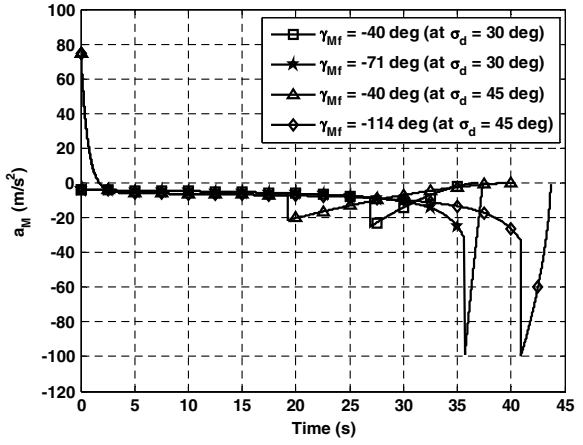

c) Lateral acceleration profiles

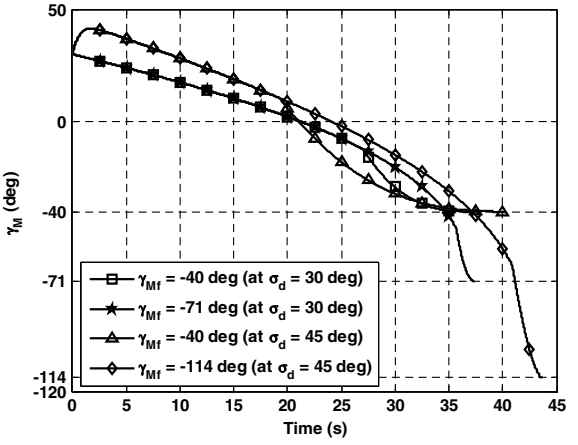

d) Flight-path angles

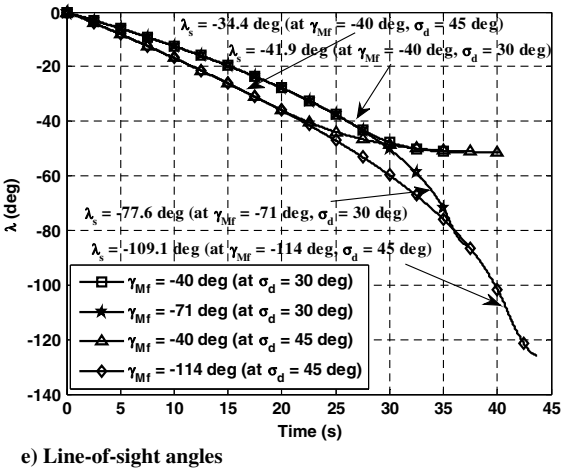

e) Line-of-sight angles

Fig. 7 Results for various impact angles and desired look angles.

trajectories in the initial phase should be shaped as spiral ones. From [16], DPP is possible to generate the spiral trajectory if $\eta < 1$ and $|\sin \sigma_d| > \eta$. Also, the desired look angle should meet Eq. (26) for $\dot{\lambda} < 0 \forall t \in [t_0, t_s]$. Therefore, the desired look angle can be selected as

$$\sin^{-1}\eta < \sigma_d < \sigma^*_{\max} \tag{38}$$

where $\sigma^*_{\max} = \min[\cos^{-1}2\eta, \tilde{\sigma}_{\max}]$, and $\tilde{\sigma}_{\max}$ can be determined considering the seeker's look-angle limit $\sigma_{\max}$, its margin, and the maximum AOA $\alpha_{\max}$ produced by the lateral acceleration during the homing phase.

IV. Numerical Examples

Nonlinear simulations are performed to investigate the performance of the proposed guidance scheme. First, to analyze basic properties of the proposed scheme, a constant-speed missile model is applied to the simulation environment. Second, a realistic missile model with aerodynamic and thrust profiles is considered for practical applicability. The missile launch procedure using the proposed guidance scheme is shown in Fig. 6.

A. Constant-Speed Missile Model

Simulation conditions for a constant-speed missile model are given as follows: initial relative range of $r_0 = 5000$ m; missile speed of $V_M = 200$ m/s; initial look angle of $\sigma_0 = \gamma_{M_0} = 30$ deg; navigation gain of $N = 3$; acceleration limit of $a_{\max} = 100$ m/s^2; look-angle limit of $\sigma_{\max} = \sigma_d = 30$ or 45 deg; target speed of $V_T = 50$ m/s; and target flight-path angle of $\gamma_T = 0$ or 180 deg.

1. Case 1: Various Impact Angles and Desired Look Angles

To investigate basic properties of the proposed guidance scheme, nonlinear simulations for $\gamma_{M_f} = -40$, -71, and -114 deg; and $\sigma_d = 30$ or 45 deg are performed against a moving target with $\gamma_T = 0$. From Eqs. (32) and (36), we choose $\gamma_{M_f,\max} = -71$ deg(for $\sigma_d = 30$ deg), -114 deg(for $\sigma_d = 45$ deg), and $K = 300$. The missile trajectories and the look-angle variations are shown in Figs. 7a and 7b, respectively. The corresponding lateral acceleration profiles and the flight-path angles are shown in Figs. 7c and 7d, respectively. Setting the larger desired look angle leads to more elevated trajectories. The LOS angle variations are shown in Fig. 7e, and the magnitude of $\dot{\lambda}_s$ is increased by setting high impact angles and low desired look angles. From these results, it can be seen that the proposed guidance scheme can achieve successful interception with the desired impact angle for the moving target under the missile's physical constraints.

2. Case 2: Comparative Study

The performance of the proposed guidance scheme is compared with a two-phase guidance scheme described in [6], which is summarized as

$$a_{\text{Ratnoo}} = \begin{cases} \frac{3\gamma_{M_0}}{2\pi} V_M \dot{\lambda} & \text{if } \frac{\gamma_{M_f}-\gamma_M}{\lambda_f-\lambda} < 3 \\ N V_M \dot{\lambda} & \text{if } \frac{\gamma_{M_f}-\gamma_M}{\lambda_f-\lambda} \geq 3 \end{cases} \tag{39}$$

For comparative studies, nonlinear simulations for $\gamma_{M_f} = -100$ deg are carried out, and the simulation results are presented in Figs. 8a–8d. Both schemes intercept the target with the desired impact angle within the acceleration limit. However, the scheme in [6] misses the target within the seeker's look angle, and it may lead to the mission failure for practical missiles with the seeker's look-angle

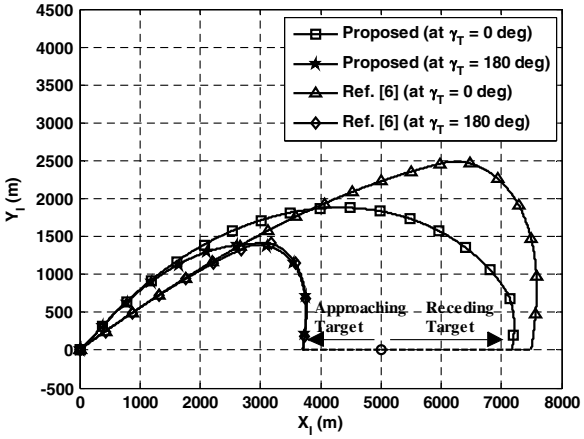

a) Missile trajectories

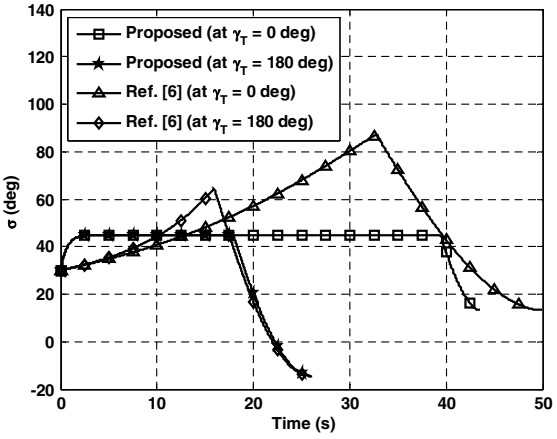

b) Look angles

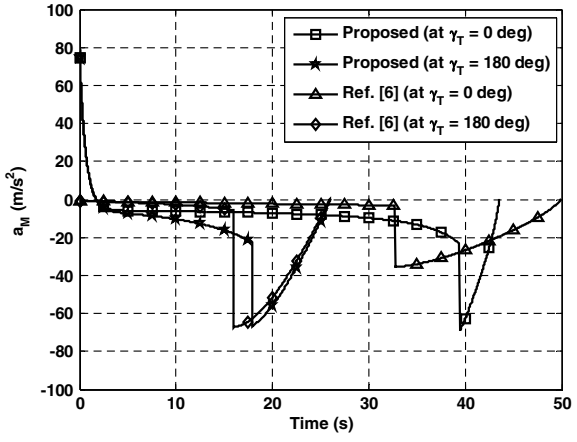

c) Lateral acceleration profiles

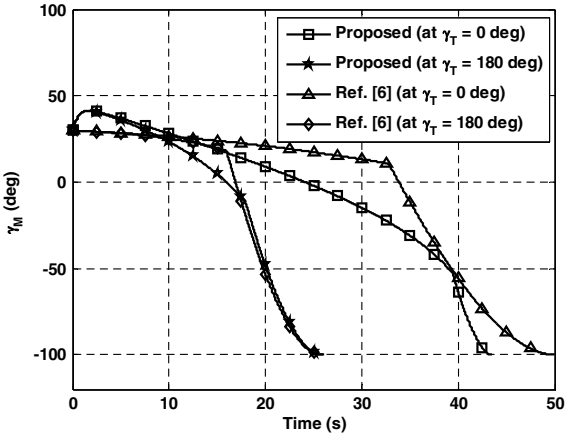

d) Flight-path angles

Fig. 8 Results for comparative study.

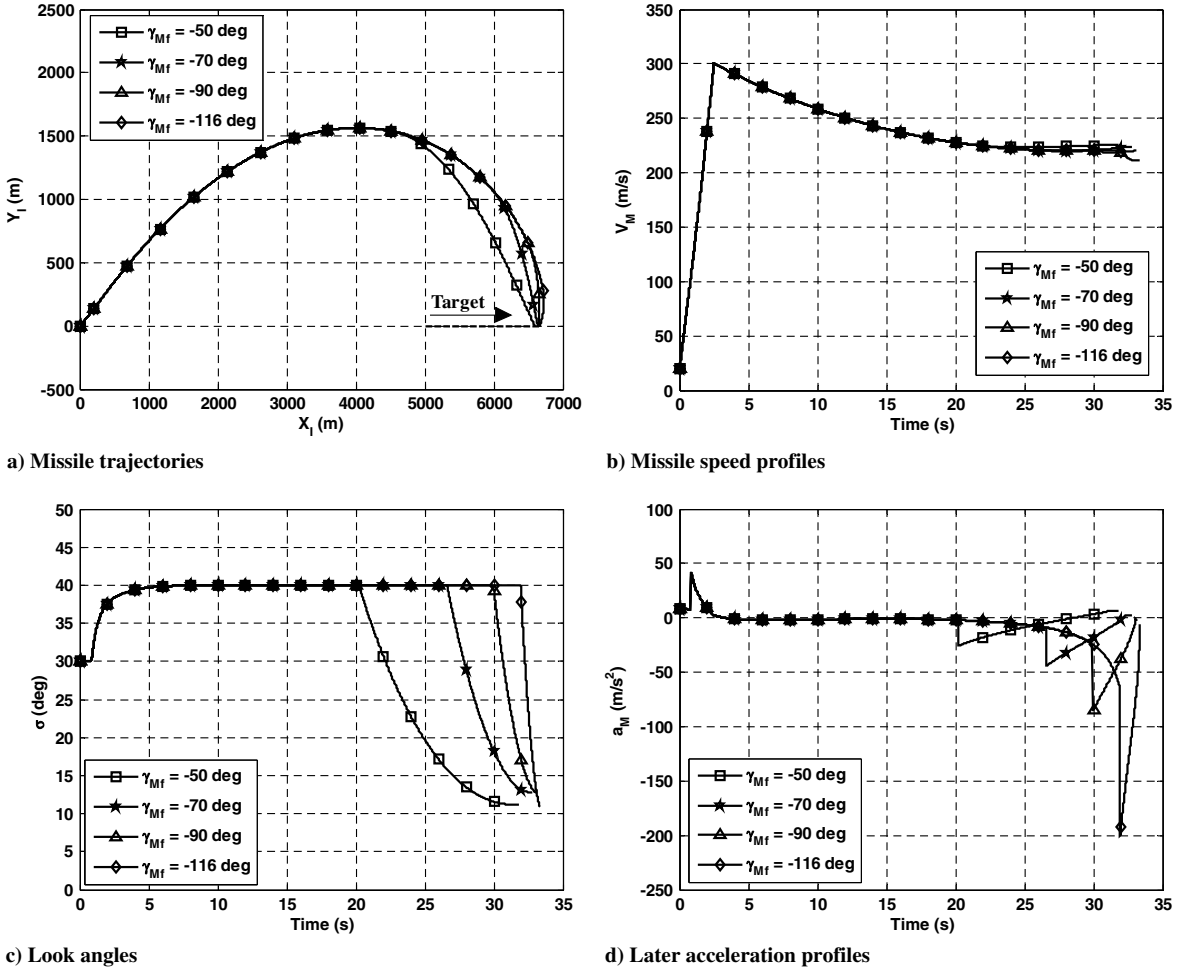

a) Missile trajectories

b) Missile speed profiles

c) Look angles

d) Later acceleration profiles

Fig. 9 Results for realistic missile model without autopilot lag.

limit. The proposed scheme successfully operates the missile against approaching and receding targets without violating the look-angle limits.

B. Realistic Missile Model

Simulation conditions for a realistic missile model are considered as follows: initial missile speed of $V_{M_0} = 20$ m/s; acceleration limit of $a_{\max} = 200$ m/s^2; desired look angle of $\sigma_d = 40$ deg; and look-angle limit of $\sigma_{\max} = 45$ deg. Other common parameters are identical to the case of a constant-speed model. Here, the aerodynamic and thrust models are taken from [17] and are modified to have an average speed of about Mach 0.7. In a realistic surface-to-surface engagement environment, gravity should be considered for generating the acceleration commands. Hence, a gravity compensation term $g \cos \gamma$, where g denotes gravity, is added to the proposed guidance command.

1. *Case 3: Lag-Free System*

The nonlinear simulations for $\gamma_{m_f} = -50, -70, -90$, and -116 deg are carried out. By applying the engagement conditions with the average speed of Mach 0.7 and gravity g to Eqs. (32) and (36), we can select $\gamma_{M_{f,\max}} = -116$ deg and $K = 200$. The missile's trajectories and its speed profiles are shown in Figs. 9a and 9b. The look angles and later acceleration profiles are shown in Figs. 9c and 9d. In the boost phase, the acceleration commands to keep the initial look-angle

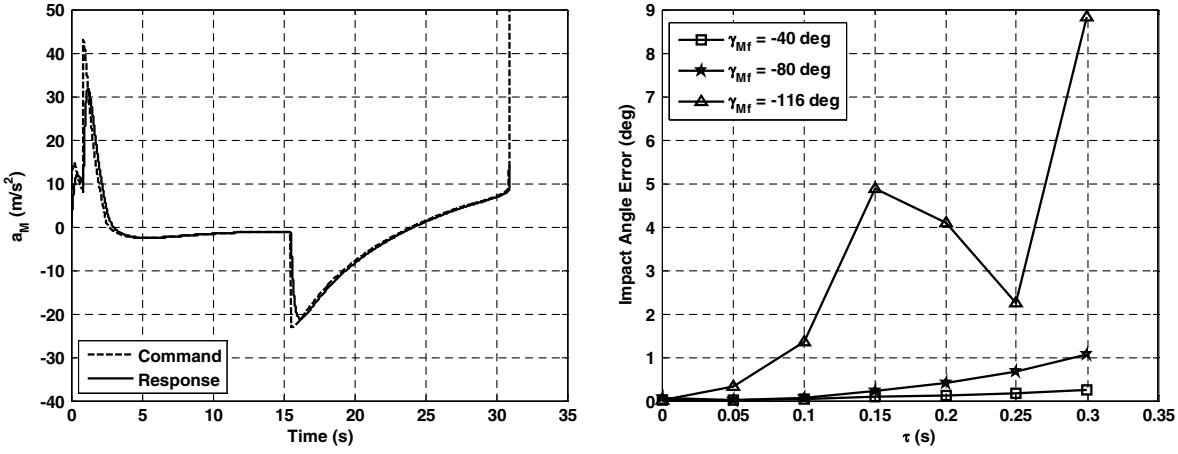

a) Lateral acceleration profiles

b) Impact angle errors

Fig. 10 Results for realistic model with autopilot lag.

constant are generated because the high maneuverability under very low speed can cause missile instability. All results show that the proposed scheme successfully impacts the target with the desired impact angle not violating the look-angle limit in the realistic environment of a surface-to-surface engagement.

2. Case 4: First-Order Lag System

The nonlinear simulations for a realistic missile model with first-order autopilot lag, where the time constant τ varies up to 0.3 s, are conducted. The lateral acceleration profiles for $\gamma_{M_f} = -40$ deg and $\tau = 0.2$ s are presented in Fig. 10a. As shown in Fig. 7b, impact angle errors for $\gamma_{M_f} = -40$ and -80 deg are less than 1.1 deg. However, the error for $\gamma_{M_f} = -116$ deg increases by 8.9 deg because the acceleration saturation, produced by the system lag during the short final phase, causes large impact angle errors at the interception instant.

V. Conclusions

A composite guidance scheme, based on the characteristics of proportional navigation, has been presented to control the impact angle against a nonmaneuvering moving target. The proposed guidance scheme is designed, considering simultaneously the seeker's look-angle and maximum acceleration limits, and has a simple structure for implementation because the two-phase guidance law has a PN form, but only different N are used as the guidance phases. In addition, calculation methods of the maximum achievable impact angle and the gain selection are described for a good guideline on operating a practical homing missile with physical constraints. The performance of the proposed guidance scheme is demonstrated through nonlinear simulations.

References

[1] Kim, M., and Grider, K. V., "Terminal Guidance for Impact Attitude Angle Constrained Flight Trajectories," *IEEE Transactions on Aerospace and Electronic Systems*, Vol. AES-9, No. 6, 1973, pp. 852–859. doi:10.1109/TAES.1973.309659

[2] Ryoo, C. K., Cho, H., and Tahk, M. J., "Optimal Guidance Laws with Terminal Impact Angle Constraint," *Journal of Guidance, Control, and Dynamics*, Vol. 28, No. 4, 2005, pp. 724–732. doi:10.2514/1.839210.2514/1.8392

[3] Ryoo, C. K., Cho, H., and Tahk, M. J., "Time-to-Go Weighted Optimal Guidance with Impact Angle Constraints," *IEEE Transactions on Control Systems Technology*, Vol. 14, No. 3, 2006, pp. 483–492. doi:10.1109/TCST.2006.872525

[4] Lu, P., Doman, D., and Schierman, J., "Adaptive Terminal Guidance for Hypervelocity Impact in Specified Direction," *Journal of Guidance, Control, and Dynamics*, Vol. 29, No. 2, 2006, pp. 269–278. doi:10.2514/1.14367

[5] Ratnoo, A., and Ghose, D., "Impact Angle Constrained Interception of Stationary Targets," *Journal of Guidance, Control, and Dynamics*, Vol. 31, No. 6, 2008, pp. 1817–1822. doi:10.2514/1.37864

[6] Ratnoo, A., and Ghose, D., "Impact Angle Constrained Guidance Against Nonstationary Nonmaneuvering Targets," *Journal of Guidance, Control, and Dynamics*, Vol. 33, No. 1, 2010, pp. 269–275. doi:10.2514/1.45026

[7] Erer, K. S., and Merttopçuoğlu, O., "Indirect Impact-Angle-Control Against Stationary Targets Using Biased Pure Proportional Navigation," *Journal of Guidance, Control, and Dynamics*, Vol. 35, No. 2, 2012, pp. 700–704. doi:10.2514/1.52105

[8] Park, B. G., Jeon, B. J., Kim, T. H., Tahk, M. J., and Kim, Y. H., "Composite Guidance Law for Impact Angle Control of Tactical Missiles with Passive Seekers," *Asia-Pacific International Symposium on Aerospace Technology*, The Korean Soc. for Aeronautical & Space Sciences, Seoul, Korea, Nov. 2012, Paper 7.1.1.

[9] Park, B. G., Kim, T. H., Tahk, M. J., and Kim, Y., H., "Composite Guidance Law for impact Angle Control of Passive Homing Missiles (in Korean)," *Journal of the Korean Society for Aeronautical and Space Sciences*, Vol. 42, No. 1, 2014, pp. 20–28. doi:10.5139/JKSAS.2014.42.1.20

[10] Park, B. G., Kim, T. H., and Tahk, M. J., "Optimal Impact Angle Control Guidance Law Considering the Seeker's Field-of-View Limits," *Journal of Aerospace Engineering*, Vol. 227, No. 8, 2013, pp. 1347–1364. doi:10.1177/0954410012452367

[11] Kim, T. H., Park, B. G., and Tahk, M. J., "Bias-Shaping Method for Biased Proportional Navigation with Terminal-Angle Constraint," *Journal of Guidance, Control, and Dynamics*, Vol. 36, No. 6, 2013, pp. 1810–1816. doi:10.2514/1.59252

[12] Tekin, R., and Erer, K. S., "Switched-Gain Guidance for Impact Angle Control Under Physical Constraints," *Journal of Guidance, Control, and Dynamics*, Vol. 38, No. 2, 2015, pp. 205–216. doi:10.2514/1.G000766

[13] Erer, K. S., Tekin, R., and Özgören, M. J., "Look Angle Constraint Impact Angle Control Based on Proportional Navigation," *AIAA Guidance, Navigation, and Control Conference*, AIAA Paper 2015-0091, Jan. 2015. doi:10.2514/62015–0091

[14] Ratnoo, A., "Analysis of Two-Stage Proportional Navigation with Heading Constraints," *Journal of Guidance, Control, and Dynamics* (to be published). doi:10.2514/1.G001262

[15] Guelman, M., "Proportional Navigation with a Maneuvering Target," *IEEE Transactions on Aerospace and Electronic System*, Vol. AES-8, No. 3, 1972, pp. 364–371. doi:10.1109/TAES.1972.309520

[16] Shneydor, N. A., *Missile Guidance and Pursuit: Kinematics, Dynamics and Control*, Horwood Publ., Chichester, England, U.K., 1998, pp. 59–67.

[17] Kee, P. E., Dong, L., and Siong, C. J., "Near Optimal Midcourse Guidance Law for Flight Vehicle," *AIAA Aerospace Sciences Meeting and Exhibit*, AIAA Paper 1998-0583, Jan. 1998. doi:10.2514/6.1998-583